ELSEVIER

Journal of Hazardous Materials 130 (2006) 155–162

Journal of Hazardous Materials

www.elsevier.com/locate/jhazmat

Assessment of the effects of release variables on the consequences of LNG spillage onto water using FERC models

Yuanhua Qiao [a], Harry H. West [a], M. Sam Mannan [a,*], David W. Johnson [b], John B. Cornwell [b]

[a] *Mary Kay O'Connor Process Safety Center, Chemical Engineering Department, Texas A&M University System, College Station, TX 77843-3122, USA*
[b] *Quest Consultants Inc., 908 26th Avenue N.W., Norman, OK 73069-8069, USA*

Available online 28 November 2005

Abstract

Liquefied natural gas (LNG) release, spread, evaporation, and dispersion processes are illustrated using the Federal Energy Regulatory Commission models in this paper. The spillage consequences are dependent upon the tank conditions, release scenarios, and the environmental conditions. The effects of the contributing variables, including the tank configuration, breach hole size, ullage pressure, wind speed and stability class, and surface roughness, on the consequence of LNG spillage onto water are evaluated using the models. The sensitivities of the consequences to those variables are discussed.

Keywords: LNG spillage; FERC model; LNG cargo tank release

1. Introduction

Liquefied natural gas (LNG) is playing an increasingly important role in the natural gas industry and energy markets. Taking the U.S. market as example, industry analysts predict that LNG imports could increase to 5% of the total U.S. gas supply by 2007 [1]. Marine transportation of LNG has been carried out with a very good safety record since 1959 [2,3]. However, the risks associated with LNG have been debated for decades. After September 11, 2001, there is a heightened sense of concern over the potential for terrorist attacks on LNG tankers. No LNG tanker or land-based LNG facility has been attacked by terrorists. However, similar natural gas and oil facilities have been favored terror targets internationally. In October 2002, the French oil tanker *Limberg* was attacked off the Yemeni coast by a bomb-laden boat [4]. The combination of recent interest in expanding or building new facilities to receive LNG carriers, along with increased awareness and concern about potential terrorist action, has raised questions about the potential consequences of incidents involving LNG marine transportation.

The major hazards of an LNG spill on water include:

1.1. Pool fires

If LNG spills near an ignition source, the evaporating gas in a combustible gas–air concentration will burn above the LNG pool (methane, the main component of LNG, burns in gas-to-air ratios between 5 and 15%). The resulting pool fire would spread as the LNG pool expanded away from its source and continued evaporating.

1.2. Flammable vapor clouds

If LNG spills but does not immediately ignite, the evaporating natural gas will form a vapor cloud that may drift some distance from the spill site. If the cloud subsequently encounters an ignition source, those portions of the cloud with a combustible gas–air concentration would burn. The vapor cloud fire would burn its way back to the LNG spill where the vapors originated, and then continue to burn as a pool fire.

1.3. Rapid phase transition or flameless explosion

The phenomenon of rapid vapor formation with concomitant loud "bangs" has been observed when LNG is released on water. This non-flaming physical interaction is referred to as "rapid phase transition (RPT)" or "flameless explosion." It is believed that the rapid phase transition will not propagate into a significantly larger damage scenario [5].

* Corresponding author. Tel.: +1 979 862 3985; fax: +1 979 458 1493.
E-mail address: mannan@tamu.edu (M.S. Mannan).

0304-3894/$ – see front matter © 2005 Elsevier B.V. All rights reserved.
doi:10.1016/j.jhazmat.2005.07.045

1.4. Confined space explosions

If significant confinement of the vapor cloud occurs after an accidental LNG release, damaging overpressures (explosion) may occur.

In this paper, we focus on the flammable vapor clouds dispersion process. The related processes, including LNG spillage and pool spread and evaporation, are also being considered. The effects of tank conditions, release scenarios, and environmental conditions on the LNG spillage, spread, and dispersion processes are evaluated.

2. Background

2.1. Experimental test for LNG spillage onto water

Quantitative data began to emerge from the Lake Charles experimental project in the 1950s. In 1968 and 1969, the U.S. Bureau of Mines Safety Research Center at Pittsburgh conducted LNG spill tests up to about 16.6 ft^3 (0.47 m^3) on a quiescent pond [6,7]. Esso Research and Engineering Company carried out LNG spillage on water tests to obtain the downwind dispersion data characteristics of a marine environment [8]. Most of the tests were conducted at two sizes—about 250 gal and about 2500 gal. In 1980, Maplin Sands tests, involving spilling quantities of refrigerated gas of up to 20 m^3, were performed by the National Maritime Institute and were sponsored by Shell to obtain dispersion and thermal radiation data [9]. The Burro tests were conducted by the Lawrence Livermore National Laboratory and the Naval Weapons Center in 1980 [10]. A total of nine LNG releases onto water were performed, with spill volumes ranging from 24 to 39 m^3. In 1987, the Falcon tests were conducted in Nevada to provide a database on LNG vapor dispersion from spills involving obstacles and to assess the effectiveness of vapor fences for mitigating dispersion hazards [11]. The highest spillage volume during the tests was 66.4 m^3.

2.2. LNG source term calculations

Fay [12] presented two models to assess the LNG release processes from the cargo tank ruptures, one for scenarios with holes above the seawater level, and the other for scenarios with holes below seawater level. Further analysis in his paper was based only on the former model.

In May 2004, under contract with the Federal Energy Regulatory Commission (FERC), ABS Consulting Inc. developed consequence assessment methods for incidents involving releases from LNG carriers [3]. FERC [13] updated the ABS report in June 2004. An orifice model was used in the ABS/FERC report to evaluate the rate of LNG release from the tank. Currently, almost all authors use the orifice model, but variations exist in assumed initial conditions and orifice coefficient.

2.3. LNG vaporization rate on water

LNG vapor generation is calculated based on the heat transferred from the water into the spilled LNG pool. In Otterman's model [2], which is the most widely accepted LNG evaporation model, the vaporization rate of 0.04 lb ft^{-2} s^{-1} (that is about 0.20 kg m^{-2} s^{-1}) was based upon the experimental data from the Bureau of Mines. Sometimes vaporization rates were reported as thickness regression rates, with a typical value of 1 in min^{-1}. Opschoor derived an evaporation rate of 0.01 lb ft^{-2} s^{-1} (0.05 kg m^{-2} s^{-1}) from the convective heat flux equations [14]. However, FERC recommended using the value of 0.034 lb ft^{-2} s^{-1} (0.17 kg m^{-2} s^{-1}), which corresponds to a heat flux of about 26,954 BTU h^{-1} ft^{-2} (85 kW/m^2) [13]. This value was obtained during the Burro tests.

2.4. LNG pool spread on water

Early spread models were based on the steady state Bernoulli equation and axi-symmetric spread on water [15,16]. With this approach, spread is driven strictly by gravity, and the rate is given as a function of pool height only. Raj and Kalelkar derived a different spreading relationship by equating gravitational force and inertial resisting force [17]. Otterman derived the spread model based on the oil spill experiment data, and concluded that those three methodologies yield almost identical predictions for the maximum pool radius [2].

Webber developed a method based on solutions of the shallow water equations and lubrication theory [18]. This approach accounts for the resistance to spreading as a result of turbulent or laminar friction. Because Webber's method has a much sound theoretical basis and accounts for friction effects, a majority of researchers believe that it is more realistic than other simpler models that ignore friction effects; thus, FERC recommended using Webber method.

Although wave action is expected to affect both the shape and rate of spread of LNG on water, little effort has been expended in defining this relationship. Quest Consultants, Inc. [19] has made some initial attempts to quantify this effect, but the lack of experimental data has made validation difficult.

2.5. Flammable vapor dispersion

Modeling of flash fires is primarily a matter of applying a dispersion model. The most well known codes to model LNG dense gas dispersion are FEM3, SLAB, HEGADAS, and DEGADIS. FEM3 is based on Navier–Stokes and the model computationally solves time-averaged, three-dimensional, turbulent transport equations that come from conservation of mass, species, momentum, and energy balances. The other three models, SLAB, HEGADAS, and DEGADIS, are one-dimensional integral models, and they use similar profiles that assume a specific shape for the crosswind profile of concentration and other properties. The downwind variation of spatially averaged crosswind values is determined by using the conservation equations in the downwind direction only.

In 1992, the American Gas Association, under provisions of 49 CFR 193, petitioned the Department of Transportation to specify the use of DEGADIS for calculation of the gas dispersion protection zones in the regulation. FERC also recommended

using DEGADIS to model the LNG vapor cloud dispersion process.

3. Hazard assessment methodology

3.1. FERC models for assessing LNG carrier spills on water

The orifice model was employed by FERC to assess the LNG release process. This model calculates the flow from a circular hole in the side of a cargo tank that allows the LNG to flow directly from the tank into the water, using the following equation:

$$Q = C_d \pi \rho_l R^2 \sqrt{2gH} \quad (1)$$

where Q is the mass flow rate (lb s^{-1}), C_d the discharge or orifice coefficient, ρ_l the density of LNG (lb ft^{-3}), R the radius of hull breach (ft), H the static head above hull breach (ft), and g is the gravitational acceleration (32.2 ft s^{-2}).

It is worthwhile to note that static head consists of both the liquid height and the ullage pressure. For the fixed volume release from a cargo tank, the flow rate will drop as the liquid level above the breach drops. The discharge orifice coefficient is assumed to be 0.65 as recommended by FERC.

As described in the background, Webber's method was recommended by FERC to model the LNG pool spread. A value of 85 kW/m^2 for heat flux was adopted by FERC. The DEGADIS model was employed by FERC to assess the vapor dispersion process. For flash fires, the level of concern is typically defined as the low flammability limit (LFL) for the substance. The downwind distance to LFL and the time to reach LFL were derived from the DEGADIS model.

3.2. FERC scenario for cargo tank vapor dispersion

The base scenario modeled by FERC is:

LNG properties:
- LNG composition: methane
- LNG density: 422.5 kg m^{-3} (26.38 lb ft^{-3})

Release scenario:
- Volume of vessel: 883,000 ft^3 (25,000 m^3)
- Percent of cargo tank volume spilled: 50%
- Total spill quantity: 441,500 ft^3 (12,500 m^3)
- Hole diameter: 3.3 ft (1 m)
- Initial liquid height above hole: 43 ft (13 m)
- Pool shape: semi-circular

Environmental conditions:
- Air temperature: 71 °F (22 °C)
- Relative humidity: 70%
- Wind speed: 6.7 mph (3.0 m/s) and 4.5 mph (2.0 m/s)
- Pasquill–Turner stability class: D and F
- Surface roughness: 0.03 ft (0.01 m)
- Averaging time: 1 min

Heat transfer parameters:
- Film boiling heat flux to pool: 26,900 BTU h^{-1} ft^{-2} (85 kW/m^2)
- Evaporation mass flux: 0.034 lb ft^{-2} s^{-1} (0.17 kg m^{-2} s^{-1})

Table 1
Computed results using FERC methodology for LNG release base scenario

Parameters	FERC results
Initial spill rate	7600 lb/s (3400 kg/s)
Total spill duration	51 min
Maximum pool radius	418 ft (127 m)
Wind speed and stability class	6.7 mph (3.0 m/s) and D stability
Downwind distance to LFL	6500 ft (2000 m)
Time LFL reaches maximum distance	16 min
Wind speed and stability class	4.5 mph (2.0 m/s) and F stability
Downwind distance to LFL	11,000 ft (3400 m)
Time LFL reaches maximum distance	29 min

The results of LNG pool spreading and vapor dispersion for the above scenario were reported by FERC as shown in Table 1.

3.3. WinFERC model for scenario assumptions sensitivity analysis

The FERC/ABS spill/spread models are employed in this paper to analyze the sensitivity of scenario assumptions to the LNG hazard assessment. A Fortran program was developed to compute the spill and spread of LNG on water and to produce a suitable input file for use with the DEGADIS vapor dispersion model. The Fortran program was carefully tested against the results produced by the MathCad version of the FERC/ABS report. This model, which will be referred to as WinFERC, was used to perform the portions of the parametric study dealing with the spill and spread of LNG on water. The WinFERC interface is shown in Fig. 1.

The vapor dispersion process is then modeled by DEGADIS model, with the data provided by WinFERC as input to DEGADIS.

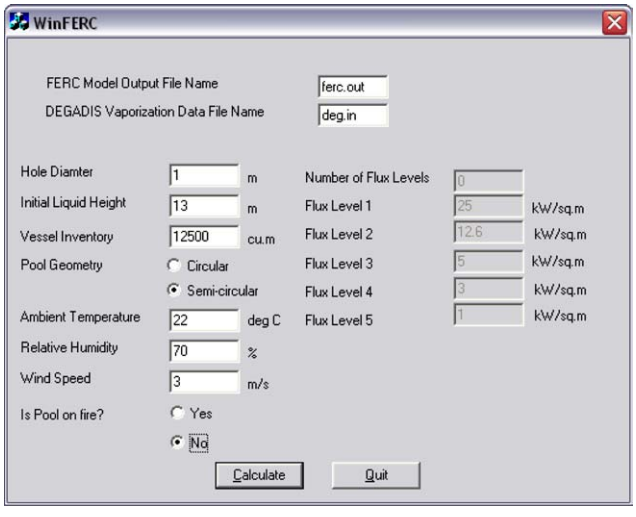

Fig. 1. WinFERC model interface.

The effects of different scenarios and assumed variables on the LNG hazard assessment results, especially the hazardous vapor cloud dispersion, are analyzed by using WinFERC and DEGADIS models. The variables analyzed include breach diameter, ullage pressure, weather conditions, and surface roughness. The base scenario modeled in this paper is the same as the FERC scenario as described in Section 3.2. During the sensitivity analysis processes, almost all the variables are the same as those in the base FERC scenario, and change is only allowed for the variable that is under sensitivity analysis, or unless specified.

4. Sensitivity of scenario assumptions on the LNG hazard assessment

4.1. Breach diameter

The results shown in Figs. 2 and 3 illustrate the effects of breach diameter on the release results, including the time to empty vessel and pool size. The time to empty vessel decreases dramatically with the increase of hole diameter as shown in Fig. 2. In Fig. 3, initially the LNG pool radius increases in correlation with increases in the breach diameter, but the pool radius reaches an asymptotic value when the breach diameter is larger than 5 m.

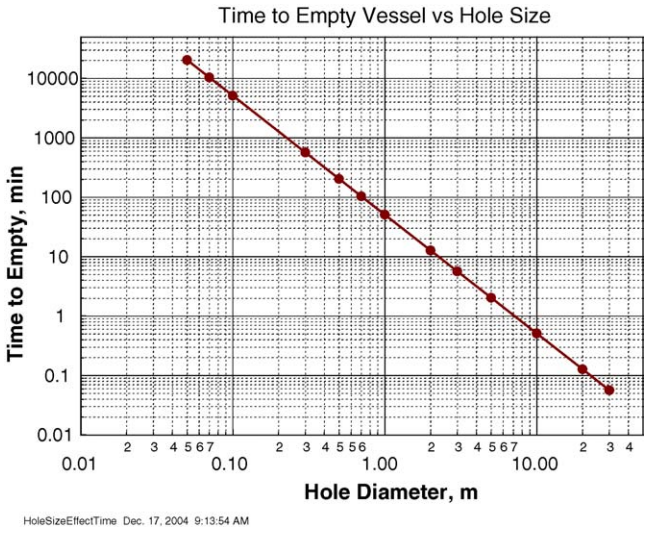

Fig. 2. Time to empty vessel vs. hole diameter.

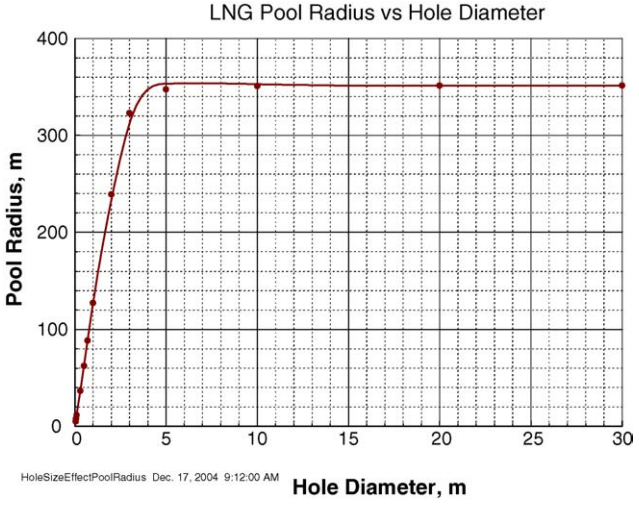

Fig. 3. LNG pool radius vs. hole diameter.

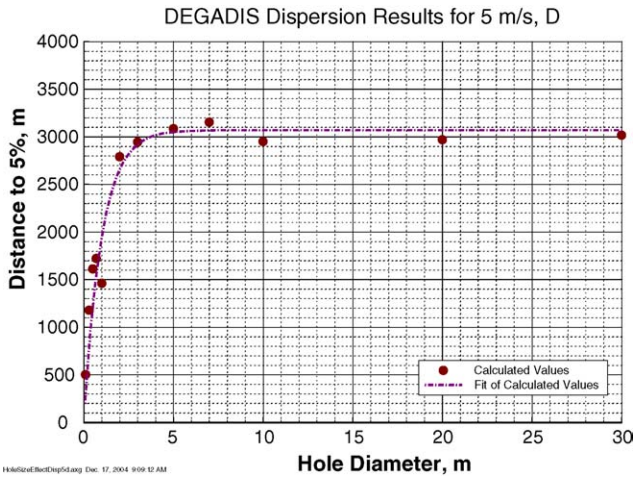

Fig. 4. LNG vapor dispersion results at 5 m/s wind speed and D stability.

Figs. 4 and 5 also show the effect of breach diameter on the LNG vapor dispersion process at two sets of atmospheric conditions. The distance to reach LFL follows a similar curve as the LNG pool radius.

4.2. Wind stability class and wind speed

Figs. 4 and 5 illustrate that the LFL downwind distance increases when the wind stability class changes from D to F and the wind speed decreases from 5 to 2 m/s. When the wind stability class transforms from neutral class D to moderately stable class F, the atmospheric turbulence tends to be weak, so that the LFL downwind distance increases. The decrease of wind speed also diminishes the turbulence level to some degree, so the LFL

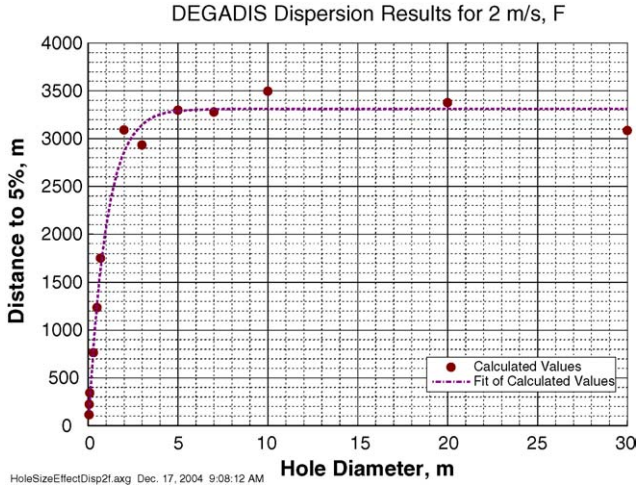

Fig. 5. LNG vapor dispersion results at 2 m/s wind speed and F stability.

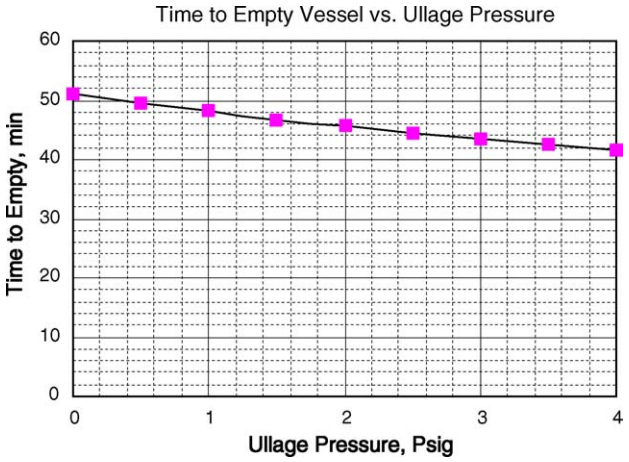

Fig. 6. Time to empty vessel for spilled LNG vs. ullage pressure.

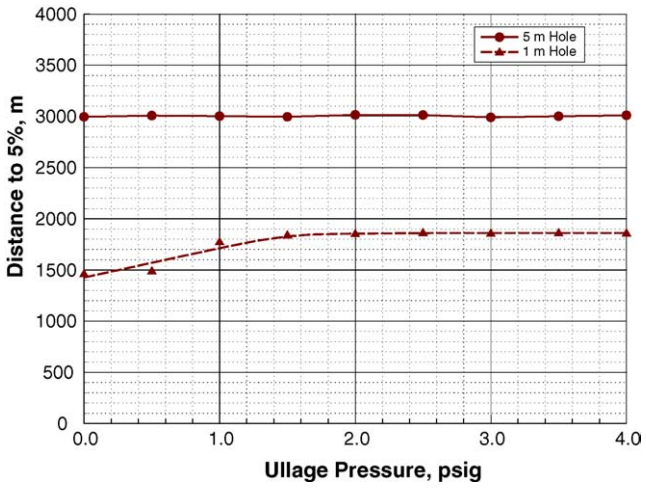

Fig. 8. LNG vapor dispersion vs. ullage pressure.

downwind distance is increased. The difference in Figs. 4 and 5 presents the combined effects of wind stability and speed on the LNG vapor dispersion process. It is interesting to note that, although the distances to the LFL at small breach diameters are different, the LFL distances for breach diameters above 5 m are similar.

4.3. Cargo tank ullage pressure

The cargo tank ullage pressure in an LNG tanker is usually less than 2 psig. For sensitivity assessment purpose, the maximum ullage pressure considered here is 4 psig. According to Eq. (1), the spill rate is proportional to the square root of static head above the breach, thus, the time to empty vessel decreases with an increase of ullage pressure, as shown in Fig. 6. Fig. 7 illustrates that the pool radius is enlarged with the increase of ullage pressure. The vapor dispersion process is also influenced by the change of ullage pressure. As shown in Fig. 8, when the hole diameter is 1 m, the LFL downwind distance is increased as the ullage pressure is increased from 0 to 2 psig, but LFL downwind distance is not strongly affected when ullage pressure is higher than 2 psig. For LNG released from 5 m diameter hole, the LFL downwind distance remains constant with the increase of ullage pressure.

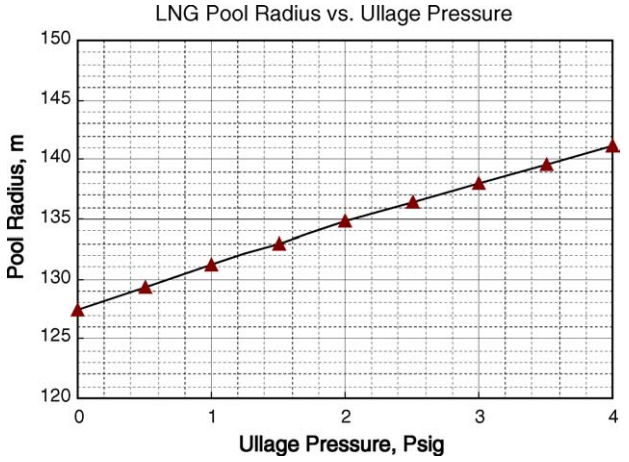

Fig. 7. LNG pool radius vs. ullage pressure.

4.4. Surface roughness

Fig. 9 illustrates the effect of surface roughness on the dispersion. When the surface roughness is high, the LFL downwind distance is decreased with the increase of surface roughness. However, when the surface roughness is less than 0.003 m, there is little change in the distance to reach the LFL. We could expect that the increase in surface roughness would increase the degree of atmospheric turbulence near grade, which would decrease the downwind extent of vapor clouds that would form and disperse near grade. Such kind of influence is similar to that of atmospheric stability. Based on the DEGADIS model calculations, the initial gravity that induced spreading of the heavy LNG vapors might overwhelm the changes in surface roughness below a roughness level of 0.003 m.

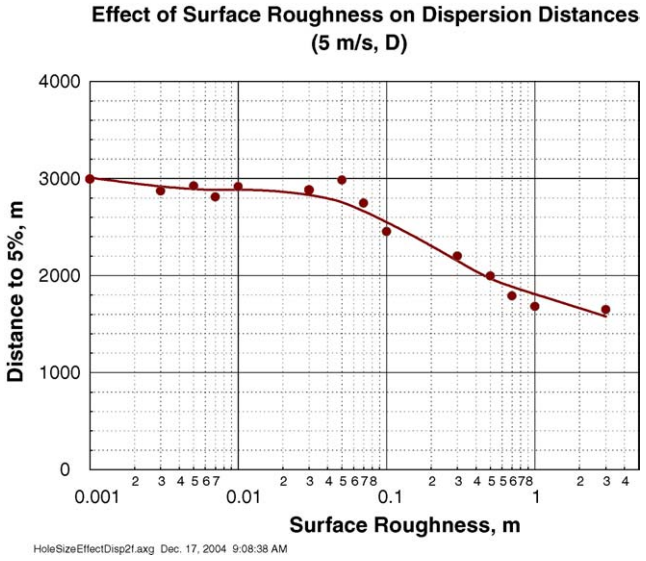

Fig. 9. Effect of surface roughness on dispersion distances.

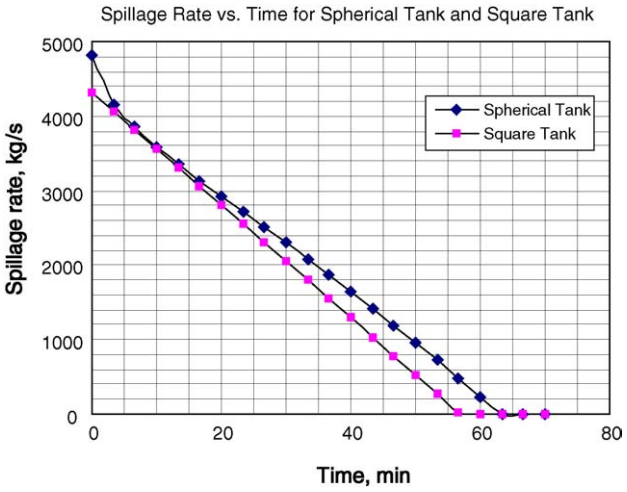

Fig. 10. Spillage rate vs. time for spherical tank and square tank.

4.5. Tank configuration

A typical membrane square tank and a typical Moss spherical tank were analyzed to determine the effect of tank configuration on the spillage process. The implicit tank configuration in most consequence analysis software is cylinder or square, with a constant cross-sectional area. The spill of LNG from a spherical tank cannot be assessed by this kind of software. The commercial program MatLab was used to compare the spillage difference for a membrane square tank and a Moss spherical tank.

The typical modern size of LNG vessels is 135,000 m^3 in four to six cargo tanks, so here a cargo tank volume of 25,000 m^3 is assumed. The diameter is 36.28 m for a Moss spherical tank, and the height is 29.24 m for a membrane square tank. The breach is assumed to be 30% from the bottom of each tank, resulting in an initial liquid level of 10.88 m above tank bottom for a spherical tank and 8.77 m for a square tank. So, the initial liquid height above breach hole is 25.4 m for a spherical tank and 20.47 m for a square tank. By running the MatLab program, the spill rates versus time for these two kinds of tanks are modeled, and the results are shown in Fig. 10.

The initial spill rate is higher for a spherical tank because of its higher static head above hull breach. The spill process is determined by the tank geometry. The spill rate decreases linearly with time for a square tank, while for a spherical tank, the spill rate decreases very quickly at the beginning, and decreases a little slowly after that.

5. Discussion

5.1. Model validation against available experimental test data

Experimentation has generally been performed on a fairly small scale. The largest spillage volume to date was 66.4 m^3, which was also the largest scale tested during Falcon tests in 1987 [11]. However, the consequence models validated with these small-scale experimental data are being used for spill scenarios of 25,000 m^3 and larger. It has been stated by Jones and McGugan that the minimum area required to enable a spill to be scaled up reliably to the dimensions of a realistic spill of 10 meters across is 1 m^2 [20]. The scale up factor of more than 350–1 (25,000–66.4 m^3) in LNG spill modeling process has left the scale up process under question for its reliability.

As a number of experiments were performed at small-scale and their relevance to real-life large spills is uncertain, a reasonable scale up factor needs to be determined and evaluated so that it is possible to test models, and subsequently, to permit any necessary modification based on the data gathered from a series of carefully controlled experiments that are at an adequately large scale.

5.2. LNG spillage process

It can be seen from Eq. (1) that the mass flow rate is a direct function of the square root of the static head, the area of the breach hole, and the discharge coefficient.

A value of 1.0 for the discharge coefficient, which is for ideal frictionless case, is not reasonable in the case of a rough, irregular hole that would be expected in a spill from an LNG carrier. The International LNG Alliance and the International Gas Union have suggested a value of 0.65, and the Center for LNG suggested a reasonable, conservative estimate of discharge coefficient ranges from 0.6 to 0.8, thus, FERC recommended 0.65, which can be defended as a reasonable estimate [13].

In this paper, a hole diameter of 1 m is selected as the base release scenario. The hazard identification team in DNV has postulated that 0.25 m is a credible hole diameter for a puncture type event, the maximum credible hole from accidental operational events will be 0.75 m, and 1.5 m from terrorist events [21]. With the hole size changing in a wider range, from 0.5 to 30 m, Fig. 2 illustrates that the time to empty the vessel changes linearly with the logarithm of the hole size as determined by Eq. (1).

The static head incorporates both the liquid height above the breach and the ullage pressure in the tank. The ullage pressure is dependent on the LNG composition and cargo tank design, and can vary from about atmospheric pressure to about 2 psig. The time to empty the vessel is approximately a linear function of the ullage pressure as shown in Fig. 6. The assumed location of the breach opening will affect the time to empty the vessel in the same way, since the breach location will determine the liquid height given the fixed tank volume and configuration. Most analysts assume the breach occurs at the waterline for modeling purpose.

The tank configuration is not a direct factor in computing the release rate in Eq. (1), but it does have an effect on the release scenario as shown in Fig. 10. The spill rate can be expressed as $Q = \rho \times dV/dt = \rho \times A \times dh$. A is uniform for the square tank, while for a spherical tank, A changes during the whole release process. The cross-sectional area is so small at the top of the spherical tank that the height drops rapidly initially and the spill rate declines quickly at the beginning. The cross-sectional area in the middle of the tank becomes larger and changes less, so the spill rate declines more slowly than the beginning.

5.3. Sensitivity of pool spreading process

The LNG will spread on the water and continuous evaporation will take place if LNG spillage occurs. The LNG pool will continue to spread until the minimum layer thickness corresponding to the maximum pool diameter is reached. The vapor production will increase during the spreading simply by virtue of the increasing area of the evaporating liquid. This will reach a maximum when the pool has reached a size corresponding to the equilibrium LNG quantity.

Otterman described the spreading process for an axisymmetric pool through the following equation [2]:

$$\frac{dr}{dt} = [2g\Delta_1 h]^{1/2} \quad (2)$$

where $h = \frac{V}{\pi r^2}$, V is the LNG volume on water (ft^3), r the pool radius (ft), $\Delta_1 = \frac{\rho_1 - \rho}{\rho_1}$, ρ_1 the density of water ($lb\,ft^{-3}$), ρ the density of LNG ($lb\,ft^{-3}$), and g the gravitational acceleration ($32.2\,ft\,s^{-2}$).

Through this equation, spread is driven only by gravity and the pool reaches the maximum with the pool layer thickness at the minimum. Webber's method accounts for the friction effects, and the maximum pool size should occur when the pool is in the minimum thickness and the gravity driven force and the turbulent or laminar resistance force are in equilibrium.

For a long-term release, the pool will spread until the evaporation rate matches the rate of spillage. Thus, the detailed modeling of pool spreading is not necessary. The pool area can be estimated from the spill rate divided by the evaporation rate per unit area.

The change of maximum pool size with the hole size in Fig. 3 can be explained by the combined effects of long-term release scenario and instantaneous spill scenario. When the breach hole diameter is less than 4 m, the LNG spillage can be viewed as long-term release process. With the hole size becoming larger, the spill rate is higher, resulting in a larger pool. When the breach hole diameter is larger than 4 m, the spill process can be simplified as instantaneous spill, and the maximum pool size is independent of the hole size.

As illustrated in Fig. 6, when the tank ullage pressure is less than 4 psig and the breach hole diameter is 1 m, the time to empty the vessel declines linearly with the ullage pressure. The spill process can be assumed as long-term release when tank ullage pressure is less than 4 psig. The increment of the ullage pressure increases the spill rate, so the maximum pool size increases with the increasing of ullage pressure accordingly.

5.4. Sensitivity of vapor dispersion process

It was found by Blackmore et al. that plume dispersion behavior is dependent on source conditions, especially for continuous LNG spills [9]. The results illustrated in Figs. 4 and 5 prove that the hole size and ullage pressure affect the dispersion process.

Increasing breach hole size and ullage pressure has similar effects in enlarging the spreading pool. A larger pool size means that the overall evaporation rate will increase. As the evaporation rate increases, the downwind distance to a given concentration increases. When the increase of the spill rate cannot enlarge the pool size and the subsequent evaporation rate, the downwind distance to LFL will not change any more as shown in Figs. 4, 5 and 8.

The wind stability class is an indicator of atmosphere turbulence level. A higher turbulence level will increase the dilution of the LNG plume with the air. So the downwind distance to LFL will increase when the turbulence level degrades. The decrease of the surface roughness and the wind speed have the similar effects on the vapor dispersion process. In Maplin Sands tests, liquid propane was continuously released from a tank at an average spill rate of $2.3\,m^3$/min. When the wind speed is 5.5 and 3.8 m/s, the observed dispersion distances to LFL were 215 and 400 m, respectively [9]. The same trend has been found in our model results shown in Figs. 4 and 5.

6. Conclusions

When an LNG cargo tank is ruptured, the LNG flows out of the hole onto the surface of water, in an amount and at a rate depending on the tank size, dimension, location of the rupture, and ullage pressure. The spilled fluid spreads on the water surface, eventually evaporating entirely, mixing with air and dispersing downwind.

The FERC modeling algorithms were employed in this paper to analyze the LNG spillage consequences. The computed results illustrate that the changes of breach size and ullage pressure will change not only the spill duration and pool size, but also the dispersion process. Variations of tank configuration affect the spill process. The wind stability, wind speed, and surface roughness affect the vapor dispersion process for breach diameters less than 4 m, but have a smaller effect on spills from breach diameters larger than 5 m.

References

[1] California Energy Commission, Liquefied Natural Gas in California: History, Risks, and Siting, http://www.energy.ca.gov/reports/2003-07-17_700-03-005.PDF, July 2003.
[2] B. Otterman, Analysis of large LNG spills on water. 1. Liquid spread and evaporation, Cryogenics 15 (8) (1975) 455.
[3] ABS Consulting, Inc., Consequence Assessment Methods for Incidents Involving Releases from Liquefied Natural Gas Carriers, May 2004.
[4] P. Parfomak, Liquefied Natural Gas (LNG) Infrastructure Security: Background and Issues for Congress, CRS Report for Congress, http://www.energy.ca.gov/lng/documents/CRS_RPT_LNG_INFRA_SECURITY.PDF, September 2003.
[5] H.H. West, Y. Qiao, M. Sam Mannan, LNG-water rapid phase transition: Part 1: A literature review, LNG J. (May 2005) 21.
[6] D.S. Burgess, J.N. Murphy, M.G. Zabetakis, Hazards Associated with the Spillage of Liquefied Natural Gas on Water, U.S. Bureau of Mines, R#17448, U.S. Department of the Interior, November 1970.
[7] D.S. Burgess, J. Biordi, Hazards of Spillage of LNG into Water, U.S. Bureau of Mines, PMSRC Report No. 4177, 1972.
[8] G.F. Feldbauer, J.J. Heigl, W. McQueen, R.H. Whipp, W.G. May, Spills of LNG on Water—Vaporization & Downwind Drift of Combustible Mixtures, Report No. EE61E-72, Esso Research & Engineering Company, November 1972.
[9] D.R. Blackmore, J.A. Eyre, G.G. Summers, Dispersion and combustion behavior of gas clouds resulting from large spillages of LNG and LPG

onto the sea, Transactions of the Institute of Marine Engineers (TM) 94, Paper 29, 1982.
[10] R.P. Koopman, R.T. Cederwall, D.L. Ermak, H.C. Goldwire, W.J. Hogan, J.W. McClure, T.G. McRae, D.L. Morgan, H.C. Rodean, J.H. Shinn, Analysis of Burro series 40-m^3 LNG spill experiments, J. Hazard. Mater. 6 (1–2) (1982) 43.
[11] S. Shin, R. Meroney, D. Neff, LNG Vapor Barrier and Obstacle Evaluation: Wind-Tunnel Simulation of 1987 Falcon Spill Series, Final report, GRI-91/0219, Gas Research Institute, March 1991.
[12] J.A. Fay, Model of spills and fires from LNG and oil tankers, J. Hazard. Mater. 96 (2–3) (2003) 171.
[13] Federal Energy Regulatory Commission, Notice of availability of staff's responses to comments on the consequence assessment methods for incidents involving releases from liquefied natural gas carriers, Docket No. AD04-6-000, June 2004.
[14] G. Opschoor, Spreading and evaporation of LNG-spills and burning LNG-spills on water, J. Hazard. Mater. 3 (3) (1980) 249.
[15] T. Enger, D.E. Hartman, Explosive boiling of liquefied gases on water, in: Proceedings of the Conference on LNG Importation and Terminal Safety, Boston, 1972.
[16] D.N. Gideon, A.A. Putnam, Dispersion hazard from spills of LNG on land and on water, Cryogenics 17 (1) (1977) 9.
[17] P. Raj, A. Kalelkar, Fire Hazard Presented by a Spreading Burning Pool of Liquefied Natural Gas on Water, Presented at Combustion Institute (USA) Western States Section Meeting, El Segundo, CA, 1973.
[18] C.J.H. van den Bosch, R.A.P.M. Weterings, Methods for the Calculation of Physical Effects (TNO Yellow Book), third ed., The Hague, The Netherlands, 1997.
[19] Quest Consultants, Inc., Modeling LNG spills in Boston Harbor, Letter from John Cornwell of Quest to Don Juckett of the U.S. Department of Energy, October 3, 2001 and Letter from John Cornwell of Quest to Clifford Tomaszewski of the Office of Natural Gas & Petroleum Import & Export Activities, November 17, 2003.
[20] C.J. Jones, P.J. McGugan, An investigation into the evaporation of volatile solvents from domestic waste, J. Hazard. Mater. 2 (1978) 223.
[21] R.M. Pitblado, J. Baik, G. Hughes, C. Ferro, S. Shaw, Consequences of LNG marine incidents, in: Proceedings of the CCPS 19th Annual International Conference, Orlando, FL, June 29–July 1, 2004.